J Mater Sci (2014) 49:2204–2212
DOI 10.1007/s10853-013-7914-4

Precipitation behaviors of carbides and Cu during continuous heating for tempering in Cu-bearing medium C martensitic steel

Jae-Gil Jung · Minsu Jung · Singon Kang · Young-Kook Lee

Received: 1 August 2013 / Accepted: 24 November 2013 / Published online: 5 December 2013

Abstract The precipitation behaviors of carbides and Cu during continuous heating for tempering were investigated in Cu-bearing medium C martensitic steel by means of dilatometry, electrical resistivity, and transmission electron microscopy. The addition of 1.5 wt% Cu suppressed carbide precipitation during quenching from 900 °C, resulting in a large amount of solute C atoms in virgin martensite. The addition of Cu increased both the finish temperature of ε-carbide precipitation and the amount of ε-carbide precipitates during continuous heating. The precipitation of cementite was retarded and the amount of cementite precipitates increased by the addition of Cu. Retarded cementite precipitation in the Cu-bearing steel was attributed to sluggish Cu partitioning from cementite particles to the martensite matrix, the hindrance to the migration of cementite interfaces by Cu particles, and the slowed diffusions of C and Fe atoms. Cu precipitation was accelerated by cementite precipitation because cementite interfaces and the high Cu concentration near cementite particles provided nucleation sites for Cu precipitation. The hardness of the tempered Cu-bearing steel was higher than that of the tempered Cu-free steel at the temperatures of over 300 °C due to both Cu precipitation hardening and retarded cementite precipitation.

J.-G. Jung · M. Jung · S. Kang · Y.-K. Lee (✉)
Department of Materials Science and Engineering, Yonsei University, Seoul 120-749, Korea
e-mail: yklee@yonsei.ac.kr

Present Address:
J.-G. Jung
Light Metal Division, Korea Institute of Materials Science, Changwon 642-831, Korea

Present Address:
M. Jung
Max Planck Institute for Intelligent Systems, 70569 Stuttgart, Germany

Present Address:
S. Kang
Advanced Steel Processing and Products Research Center, Colorado School of Mines, Golden, CO 80401, USA

Introduction

The tempering behavior of medium C steel, which has been used for the mechanical parts of machines and automobiles, has been extensively investigated because tempering is an important heat treatment for improving the toughness and ductility of quenched martensitic steels without a great loss of strength and hardness [1–9].

The tempering behavior of medium C alloyed steel is generally divided into four stages depending on the tempering temperature [6–9]. The transition ε-carbide first forms at temperatures ranging from 70 to 240 °C (stage 1), the decomposition of retained austenite occurs at temperatures between approximately 200 and 300 °C (stage 2), and cementite forms at temperatures ranging from 200 to 450 °C (stage 3) [6, 7]. At higher temperatures, alloying elements, such as Cr, Mo, W, and Ti, precipitate as fine alloy carbides at the interfaces of pre-existing cementite particles and in the tempered martensite matrix, resulting in the secondary hardening (stage 4) [8, 9].

Non-carbide-forming elements like Cu can also precipitate during the tempering of martensitic steels if their solubilities in the bcc matrix are low [10]. The kinetics of Cu precipitation has been investigated in both low [11–14] and medium [15] C steels. The isothermal precipitation of Cu in the bcc matrix of low C steels was the fastest at approximately 600 °C [11, 12], and was greatly accelerated by tensile strain [13]. Bhagat et al. [14] reported that Cu

precipitation in low C Ni-bearing steel was completed during continuous heating to 550 °C at a slow rate of 0.33 °C/s.

Meanwhile, the isothermal precipitation of Cu in medium C steel occurred at the interfaces of cementite particles as well as in the tempered martensite matrix, and was much faster than that in low C steel because cementite particles provided preferential nucleation sites for Cu precipitation [15]. Regarding Cu precipitation during continuous heating in medium C steel, there is a report stating that Cu precipitated during furnace heating to the tempering temperatures of over 450 °C [15]. However, the quantitative evaluation of the kinetics of Cu precipitation occurring during continuous heating for tempering in medium C martensitic steel has not been performed.

Alloying elements not only precipitate as alloy carbides or metals during tempering as above-mentioned, but also affect the precipitation behaviors of carbides such as ε-carbide and cementite [8, 16–19]. Ti accelerates the precipitation of ε-carbide because fine TiC particles, which already formed at high temperatures, provide preferential nucleation sites for the precipitation of ε-carbide [16]. Si stabilizes the ε-carbide, delaying the transition from ε-carbide to cementite [8]. The partitioning of alloying elements, such as Si [17–19], Mn [17, 18], Cr [17], and Ni [17], between the matrix and cementite particles decelerates the growth and coarsening rates of cementite particles, retarding the decrease in hardness of tempered martensite. However, there are few reports on the effects of Cu on the precipitation behaviors of ε-carbide and cementite in both low and medium C steels.

Therefore, in the present study we investigated the kinetics of both carbides and Cu precipitations occurring during continuous heating for tempering and the effects of Cu on carbide precipitation during both quenching and continuous heating in Cu-bearing medium C martensitic steel by means of dilatometry, electrical resistivity, and transmission electron microscopy.

Experimental procedure

Two cold-rolled medium C steels with and without Cu, whose chemical compositions are listed in Table 1, were used in the present study. Rectangular specimens measuring $1 \times 10 \times 100$ mm^3 were taken from the cold-rolled steel sheets, and were solution-treated at 900 °C for 10 min using a vacuum tubular furnace and then quenched into water of room temperature to obtain a fully martensitic microstructure without Cu particles. To confirm the existence of retained austenite in the solution-treated and water-quenched 0 Cu and 1.5 Cu steels, X-ray diffraction (XRD) tests were performed using Fe Kα radiation ($\lambda = 0.1937$ nm). The scanning angle (2θ) ranged from 55° to 130° and the scanning speed was 0.5°/min. The grain size of prior austenite of the solution-treated and water-quenched 0 Cu and 1.5 Cu steels was similar to be approximately 22 μm [15].

Table 1 Chemical compositions of medium C steels investigated in this study (wt%)

Steel	C	Mn	Si	Cu	Cr	P	S	Fe
0 Cu	0.44	0.75	0.25	–	0.03	<0.03	<0.035	Bal.
1.5 Cu	0.44	0.60	0.21	1.53	0.11	<0.03	<0.035	Bal.

Dilatometric specimens measuring $1 \times 3 \times 10$ mm^3 were taken from the solution-treated and water-quenched 0 Cu and 1.5 Cu steels. They were induction-heated up to 700 °C at various heating rates ranging from 0.1 to 50 °C/s to measure the strain change during continuous heating, and then cooled to room temperature at 10 °C/s using a dilatometer (Theta, Dilatronic III). The values of electrical resistivity of the solution-treated and water-quenched 0 Cu and 1.5 Cu specimens were measured as a function of temperature during continuous heating at 0.1 °C/s by a four-point probe method using an apparatus for electrical resistivity measurement (ULVAC-RIKO, TER-2000). The size of specimens for electrical resistivity measurement was $1 \times 10 \times 100$ mm^3 and the specimens were mechanically polished before resistivity measurement.

Precipitates were examined with carbon extraction replicas on Ni-grids using a transmission electron microscope (TEM, JEOL, JEM2100F) attached with an energy dispersive X-ray spectrometer (EDXS, Oxford, INCA Energy). In order to investigate the effect of Cu addition on mechanical property, the hardness values of tempered 0 Cu and 1.5 Cu specimens were measured five times per each sample in the C scale using a Rockwell hardness tester, and then were averaged.

Results and discussion

Carbide precipitation during quenching

Figure 1a shows the XRD patterns of both the 0 Cu and 1.5 Cu steels, which were solution-treated at 900 °C for 10 min and water-quenched. There was no retained austenite in the two steels because of the relatively high martensitic transformation start (M_s) temperatures: 380.4 °C for 0 Cu steel and 363.1 °C for 1.5 Cu steel. M_s temperatures were calculated using the following equation [20]:

$$M_s(^\circ\mathrm{C}) = 545 - 330\mathrm{C} - 23\mathrm{Mn} - 14\mathrm{Cr} - 13\mathrm{Ni} - 7\mathrm{Si} + 2\mathrm{Al} + 7\mathrm{Co} - 5\mathrm{Mo} - 13\mathrm{Cu}\,(\mathrm{wt}\%) \quad (1)$$

The peak-splitting in XRD pattern of α′ martensite was observed in both 0 Cu and 1.5 Cu steels due to its tetragonality (Fig. 1a).

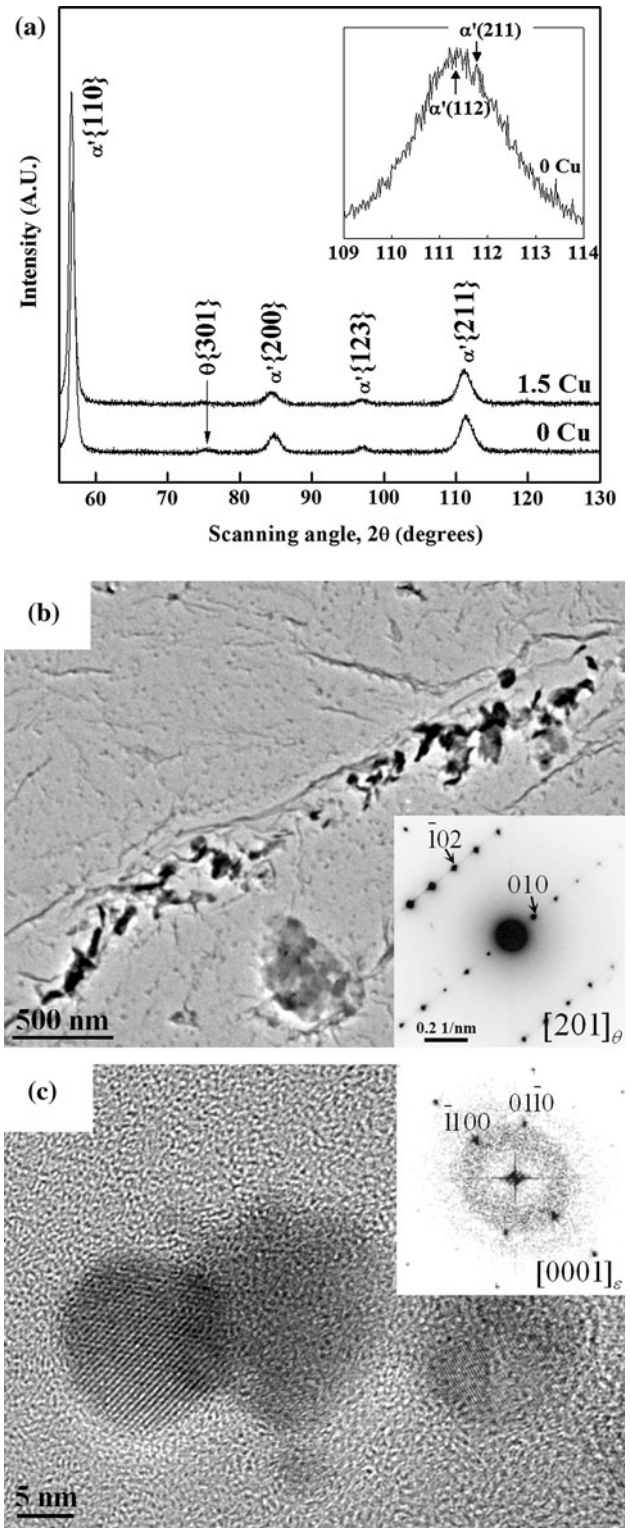

Fig. 1 **a** XRD patterns of both 0 Cu and 1.5 Cu steels, which were solution-treated at 900 °C for 10 min and then water-quenched, and TEM images showing **b** cementite (θ) and **c** ε-carbide particles, which formed during quenching from 900 °C in the 0 Cu steel

The pre-segregation of C atoms and the precipitations of ε-carbide and cementite take place even during quenching in steels with high M_s temperatures, which are referred to as auto-tempering [6, 21]. As shown in Fig. 1b, the solution-treated and water-quenched 0 Cu steel exhibited some precipitates in a row, whose size was 50–100 nm. The precipitates were identified as cementite particles from the analysis of a selected area diffraction pattern (SADP), agreeing with the XRD result (Fig. 1a). The small ε-carbide particles of approximately 10 nm were also observed in the solution-treated and water-quenched 0 Cu steel (Fig. 1c). This carbide precipitation indicates that auto-tempering occurred during quenching in the 0 Cu steel. Meanwhile, the solution-treated and water-quenched 1.5 Cu steel revealed neither cementite nor ε-carbide, indicating that auto-tempering was significantly suppressed by the addition of Cu. This is most likely due to both the lowered M_s temperature and the slowed diffusions of C [22] and Fe [23] atoms in the bcc iron with increasing the Cu concentration.

Precipitations of ε-carbide and cementite during continuous heating

Figure 2a shows variations in dilatometric strain (ε) and its derivative ($d\varepsilon/dT$) with temperature measured during continuous heating to 600 °C at 0.1 °C/s in the solution-treated and water-quenched 0 Cu steel. The dilatometric curve shows the contraction twice. The first decrease in dilatometric strain occurred between 97 and 186 °C, corresponding to the tempering stage 1, where ε-carbide precipitates [6]. The second decrease in dilatometric strain occurred between approximately 220 and 400 °C, corresponding to the tempering stage 3, where cementite precipitates [6]. These temperature ranges, at which carbides formed, were consistent with those on the curves of derivatives of both strain ($d\varepsilon/dT$) (Fig. 2a) and electrical resistivity ($d\rho/dT$) (Fig. 2b). Meanwhile, the increase in the ($d\rho/dT$) value was observed at temperatures of below 100 °C, as shown in Fig. 2b. This is most likely due to the clustering of C atoms before the precipitation of ε-carbide, which causes the severe lattice distortion of martensite, finally increasing the electrical resistivity [5].

Contractions on the dilatometric curve by the precipitations of ε-carbide and cementite were also observed in the solution-treated and water-quenched 1.5 Cu steel. The first contraction occurred at temperatures ranging from 106 to 211 °C and the second one took place at temperatures ranging from 242 to 422 °C (Fig. 2c). The amounts of strain changes by the precipitations of both ε-carbide and

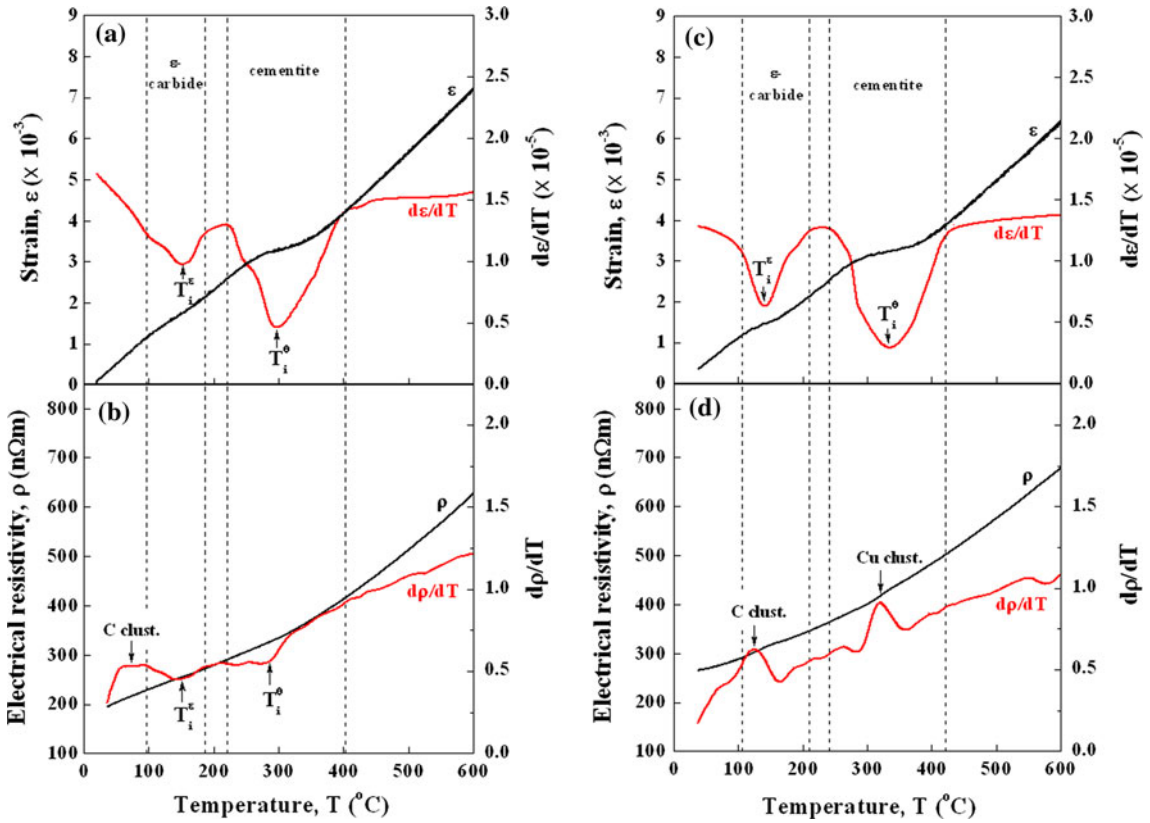

Fig. 2 Variations in **a**, **c** dilatometric strain, **b**, **d** electrical resistivity, and their derivatives (dε/dT or dρ/dT) with respect to the temperature of **a**, **b** 0 Cu and **c**, **d** 1.5 Cu steels with continuous heating temperature at 0.1 °C/s

cementite in the 1.5 Cu steel were greater than those in the 0 Cu steel most likely due to the larger amount of solute C atoms remaining in the virgin martensite of the 1.5 Cu steel, which was caused by the suppressed auto-tempering during quenching from 900 °C.

The abrupt increase in the (dρ/dT) value was observed twice in the 1.5 Cu steel, as shown in Fig. 2d. The first increase in the (dρ/dT) value occurred at approximately 120 °C due to the clustering of C atoms, as was observed in the 0 Cu steel (Fig. 2b). The second increase in the (dρ/dT) value occurred at approximately 320 °C most likely due to the clustering of Cu atoms because C clustering was already completed and cementite precipitation decreases electrical resistivity [5].

Figure 3a shows the continuous heating precipitation (CHP) diagrams for both ε-carbide and cementite in the 0 Cu and 1.5 Cu steels. The start and finish temperatures of carbide precipitation were determined from the slope change on each (dε/dT) curve, which was obtained at a given heating rate. The critical temperatures of both ε-carbide and cementite precipitations in the two steels were shifted to higher temperatures with increasing the heating rate. Whereas the precipitation start of ε-carbide was not significantly influenced by the addition of Cu, the precipitation finish was slightly delayed with increasing the Cu concentration. Meanwhile, regarding cementite precipitation, both start and finish temperatures increased by the addition of Cu.

The activation energies for the precipitations of ε-carbide and cementite in both 0 Cu and 1.5 Cu steels were calculated using a Kissinger method (Fig. 3b) as follows [24]:

$$\ln\frac{\phi}{T_{\mathrm{i}}^2} = -\frac{Q}{RT_{\mathrm{i}}} + \text{const.}, \tag{2}$$

where ϕ is a constant heating rate, T_{i} is the temperature corresponding to an inflection point on the curve of the strain-derivative (dε/dT), Q is the activation energy for precipitation, and R is the gas constant, respectively.

The activation energy for the precipitation of ε-carbide (120 kJ/mol) in the 0 Cu steel was similar to that (111 kJ/mol) in 1.5 Cu steel. These activation energy values were comparable to those measured by means of differential scanning calorimetry (111 kJ/mol) and dilatometry (126 J/mol) in the Fe–1.1 wt% C martensitic steel [21]. The activation energy value for the precipitation of ε-carbide in the 0 Cu steel was in between the activation energy value for the volume diffusion of C atoms (80 kJ/mol) in the martensite matrix and the activation energy value for the

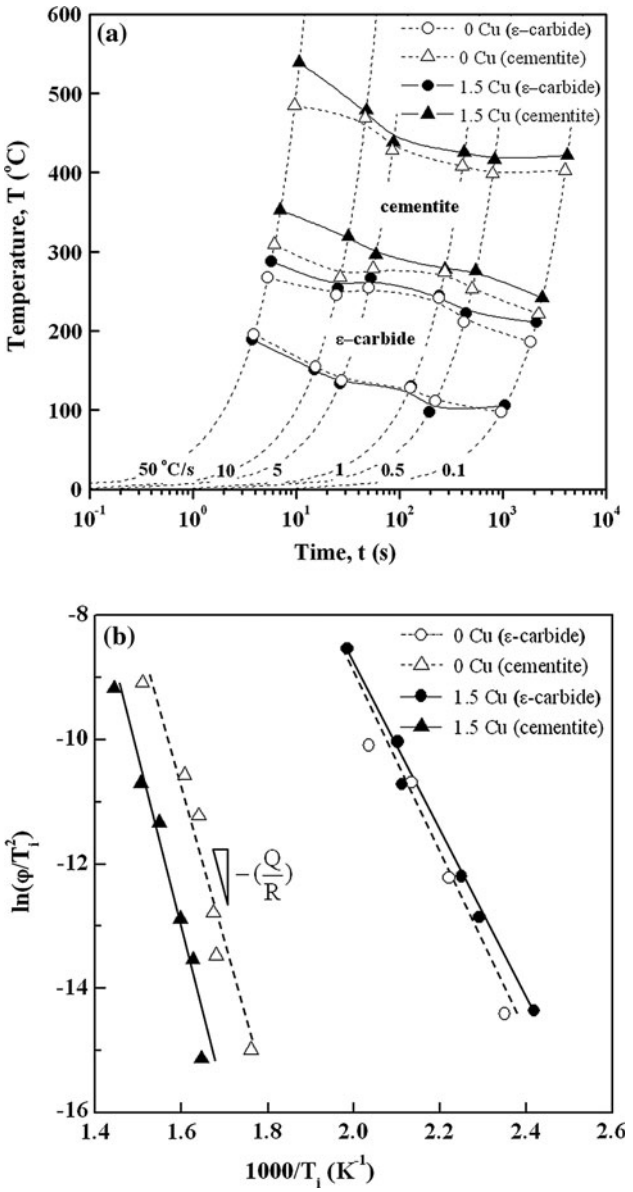

Fig. 3 **a** Continuous heating precipitation (CHP) diagrams and **b** Kissinger plots of the precipitations of ε-carbide and cementite in 0 Cu and 1.5 Cu steels, where φ is the constant heating rate, T_i is the temperature corresponding to an inflection point on the curve of the strain-derivative ($d\varepsilon/dT$), Q is the activation energy for precipitation, and R is the gas constant

pipe diffusion of Fe atoms (134 kJ/mol) in the bcc iron matrix [25].

The activation energy value for cementite precipitation in the 0 Cu steel was measured to be 206 kJ/mol, which was similar to that (203 kJ/mol) in the Fe–1.1 wt% C steel [21] and was in between the activation energy value for the pipe diffusion of Fe atoms (134 kJ/mol) [25] and the activation energy value for the volume diffusion of Fe atoms (251 kJ/mol) [26] in the bcc iron. Meanwhile, the activation energy value for cementite precipitation (225 kJ/mol) in the 1.5 Cu steel was higher compared to that (206 kJ/mol) in the 0 Cu steel, as was expected from delayed cementite precipitation by the addition of Cu (Fig. 3a).

Because the retardation of cementite precipitation and the increase in activation energy for cementite precipitation in the 1.5 Cu steel indicate the slow growth of cementite particles, the comparative observations of cementite particles in both 0 Cu and 1.5 Cu steels were performed. The two steels were continuously heated to 400 °C at the same heating rate of 5 °C/s, which corresponds to the final stage of cementite precipitation (Fig. 3a), and their microstructures are shown in Fig. 4. The size of cementite particles in the 1.5 Cu steel was smaller than that in the 0 Cu steel, as was expected. In addition, small Cu particles were observed in the vicinity of cementite particles in the 1.5 Cu steel, as shown in Fig. 4b, c.

To investigate the reasons for both the slow growth of cementite precipitates and Cu precipitation near cementite particles in the 1.5 Cu steel, the distributions of alloying elements within a cementite particle were examined with a carbon replica specimen using the TEM–EDXS. This is because it is known that the partitioning of alloying elements between the matrix and cementite particles reduces the growth and coarsening rates of cementite precipitates [17–19].

Figure 5a shows an ellipsoidal cementite particle precipitated in the 1.5 Cu steel, which was continuously heated to 400 °C at 5 °C/s and then gas-quenched. A line profile of the Cu concentration within the cementite particle (Fig. 5b) revealed that Cu atoms were enriched at the edges of the cementite particle. This implies that Cu atoms were on the move from the interior of the cementite particle to the neighboring martensite matrix because the solubility of Cu within cementite is nearly zero [27]. This Cu partitioning shows good agreement with the previous result measured by means of atom probe tomography (APT) using a pearlitic steel with less than 0.1 wt% Cu, which was annealed at 550 °C for 5 s and then cold-drawn [28], and also with the result predicted by the first-principle calculation [29]. Therefore, the sluggish partitioning of Cu atoms between the tempered martensite matrix and cementite particles is thought to reduce the growth rate of cementite particles.

Si atoms were also segregated to the edges of the cementite particle as shown in Fig. 5b, indicative of their partitioning from the interior of the cementite particle to the adjacent martensite matrix. This Si partitioning is consistent with the previous results measured in hypoeutectoid steels by means of APT [17–19]. However, the partitioning of Si atoms between the matrix and cementite particles is not thought to be responsible for retarded precipitation of cementite in the 1.5 Cu steel because the Si partitioning occurred in both 0 Cu and 1.5 Cu steels. Meanwhile, the partitioning of both Cr and Mn atoms was

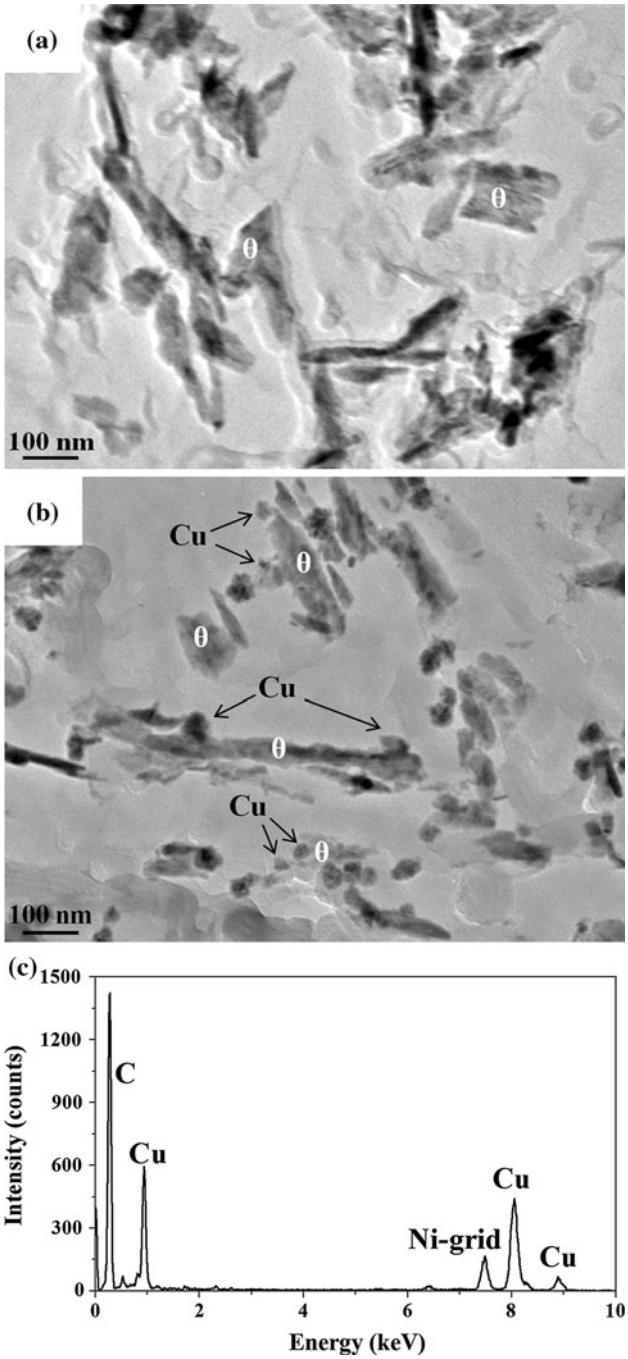

Fig. 4 TEM images showing the precipitates of cementite (θ) and Cu in **a** 0 Cu and **b** 1.5 Cu steels, which were continuously heated to 400 °C at 5 °C/s, followed by gas quenching and **c** the EDXS of the Cu particles in **b**

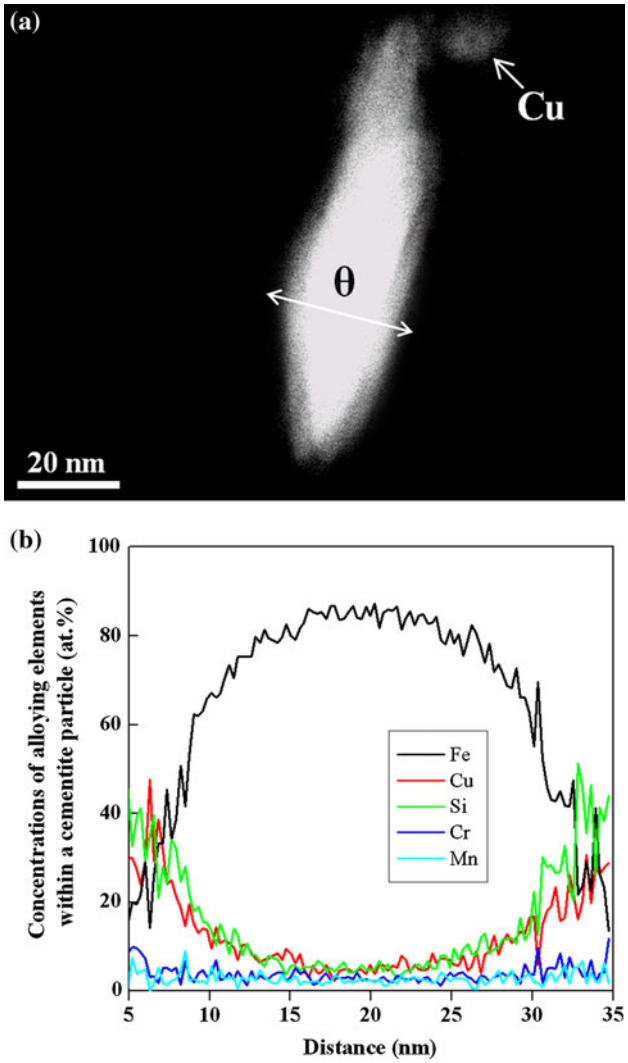

Fig. 5 **a** TEM image showing a cementite (θ) particle and a Cu particle in the 1.5 Cu steel, which was continuously heated to 400 °C at 5 °C/s, followed by gas quenching, and **b** the line profiles of the concentrations of alloying elements within the cementite particle

rarely observed in the 1.5 Cu steel (Fig. 5b), although they are expected to partition from the bcc iron matrix to the cementite particle [17, 29].

This partitioning of Cu atoms from the interior of the cementite particle to the adjacent martensite matrix made Cu-enriched regions near cementite particles, finally resulting in Cu precipitation in the vicinity of cementite particles, as shown in Figs. 4b and 5a. The Cu precipitates, which formed near cementite particles, are considered to additionally retard the growth of cementite particles by hindering the migration of the interfaces of cementite particles. Furthermore, it is thought that the diffusions of C [22] and Fe [23] atoms, which were slowed by solute Cu atoms in Cu-enriched regions near cementite particles, also delayed the growth of cementite particles.

Cu precipitation during continuous heating

Figure 6a shows an isothermal precipitation–time–temperature (PTT) diagram of Cu precipitation in the 1.5 Cu steel. The diagram was drawn using the Johnson–Mehl–Avrami (JMA) equation [30], which was obtained from the isothermal kinetics of Cu precipitation measured using the

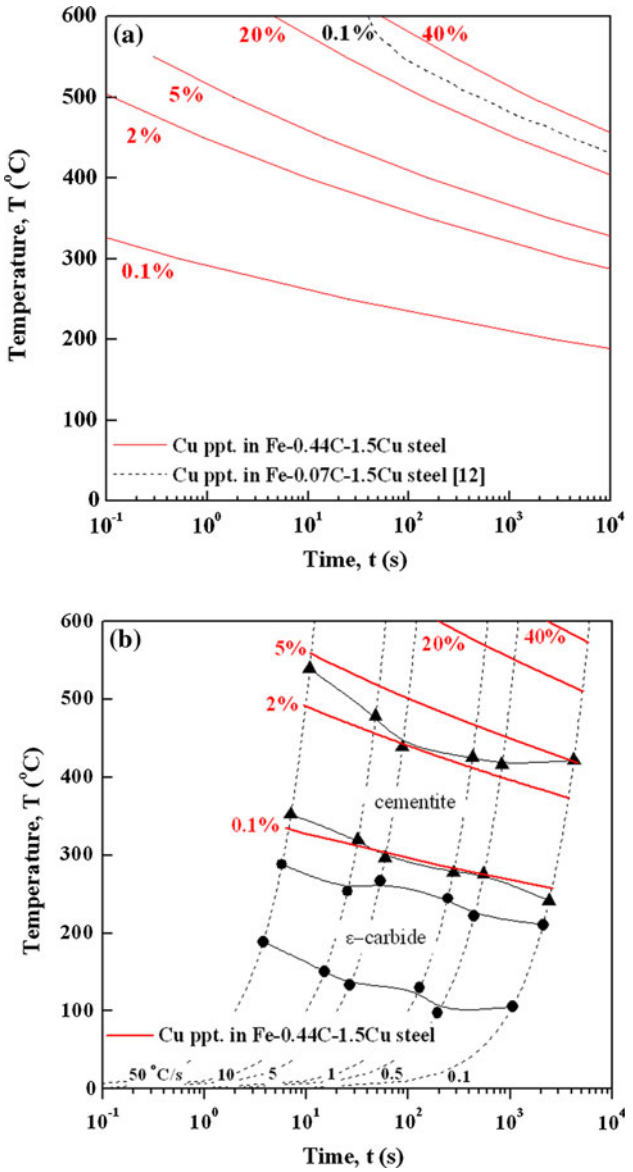

Fig. 6 **a** Isothermal precipitation–time–temperature (PTT) and **b** continuous heating precipitation (CHP) diagrams of Cu precipitation in the 1.5 Cu steel with the start curve of isothermal Cu precipitation in a low C steel [12]

1.5 Cu steel in the previous study [15]. The PTT diagram shows that the isothermal kinetics of Cu precipitation in the 1.5 Cu steel is accelerated with increasing the tempering temperature, and is faster than that in low C steel (black dotted curve in Fig. 6a) [12].

The rule of additivity [31] was used to convert the isothermal kinetics of Cu precipitation (Fig. 6a) to the kinetics of Cu precipitation during continuous heating using the following equation.

$$\int_0^{\tau^{CHP}} \frac{dt}{\tau^{PTT}(\theta(t))} = 1, \tag{3}$$

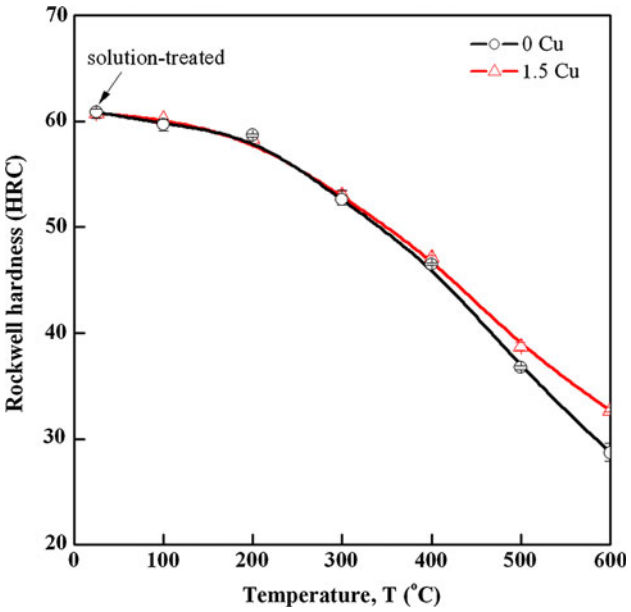

Fig. 7 Variation in hardness value with temperature in 0 Cu and 1.5 Cu steels, which were continuously heated at 5 °C/s to various temperatures and then promptly gas-quenched to room temperature

where θ is the isothermal holding temperature, $\tau^{PTT}(\theta)$ is the holding time required to obtain a specific volume fraction as a function of θ, and τ^{CHP} is the time required to obtain the same volume fraction during continuous heating at a given heating rate.

Figure 6b shows the CHP diagrams of both carbides and Cu precipitations in the 1.5 Cu steel. The diagrams show that a small amount of Cu (less than 5 %) precipitated during cementite precipitation. This is also consistent with the increase in ($d\rho/dT$) value just after the start of cementite precipitation in the 1.5 Cu steel (Fig. 2d). The fraction of Cu precipitates rapidly increased with increasing the temperature after the completion of cementite precipitation.

Figure 7 shows the change in hardness value with temperature in both 0 Cu and 1.5 Cu steels, which were continuously heated at 5 °C/s to various temperatures and then promptly gas-quenched to room temperature. The hardness values were measured at room temperature using the quenched specimens. The hardness values of the two steels gradually decreased with increasing the temperature due to the tempering of martensite [32], and were similar to each other until approximately 300 °C due to the insignificant solid-solution hardening of Cu atoms in martensite [33]. However, when the temperature became higher than 300 °C, the hardness of the 1.5 Cu steel became higher than that of the 0 Cu steel most likely due to the precipitation hardening of Cu [34, 35] as well as the delayed cementite precipitation [17–19]. TEM works were

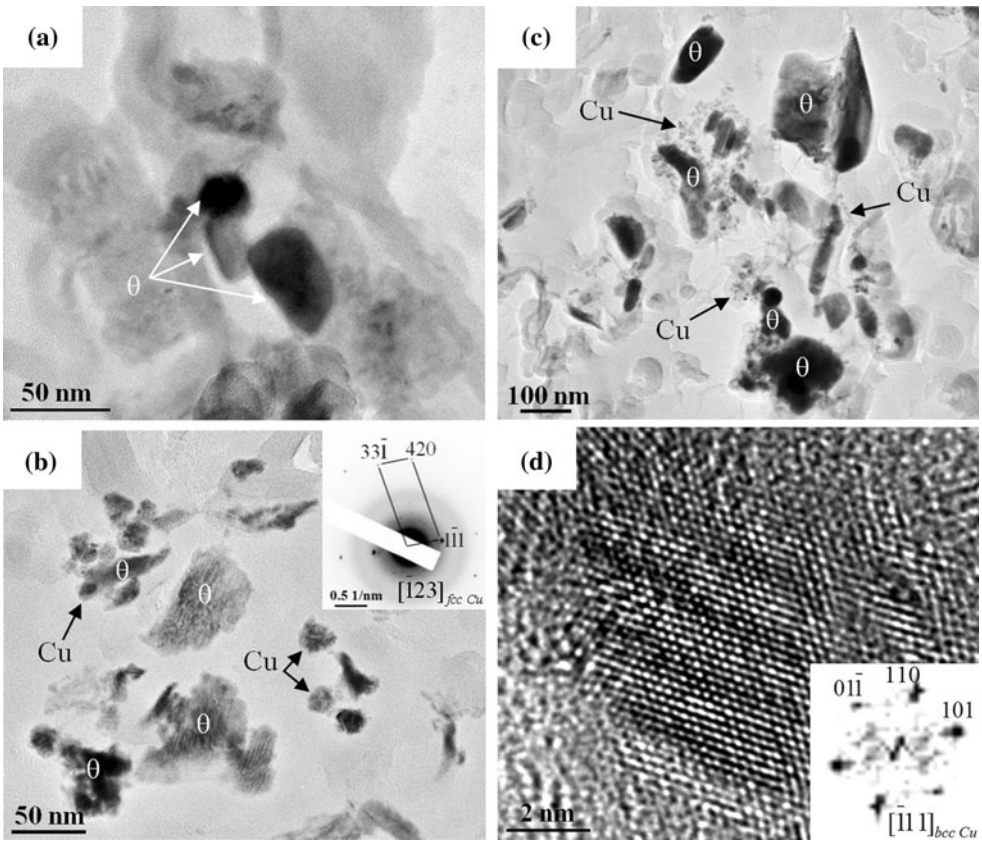

Fig. 8 TEM images showing the precipitates of cementite (θ) and Cu in the 1.5 Cu steels, which were continuously heated at 5 °C/s to **a** 300 °C and **b** 400 °C and **c** at 50 °C/s to 700 °C, followed by gas quenching, and **d** high resolution image of Cu particles in **c**

performed to validate the kinetics of Cu precipitation predicted from both the CHP diagram and the hardness result.

When the 1.5 Cu steel was heated to 300 °C at 5 °C/s and gas-quenched, only cementite particles without Cu precipitates were observed, as shown in Fig. 8a. When the temperature arose to 400 °C, both the size and fraction of cementite particles increased and fcc Cu particles started to be observed at the interfaces of cementite particles as well as in the martensite matrix (Fig. 8b). These TEM observations show good agreement with both the CHP diagram of Cu precipitation and the hardness result.

It is thought that Cu precipitation at the interfaces of cementite particles is most likely due to both the high interfacial energy [36] and Cu-enrichment near cementite particles and that this interface precipitation of Cu accelerated the kinetics of Cu precipitation in the present medium C steel, as shown in Fig. 6a. Fourlaris et al. [27] and Wasynczuk et al. [37] also reported that the interfaces of cementite particles acted as preferential nucleation sites for Cu precipitation, and that orientation relationships between fcc Cu particles and cementite (θ) particles were $[\bar{1}12]_{\text{fcc Cu}}//[\overline{111}]_{\theta}$, $(\overline{2}20)_{\text{fcc Cu}}//(312)_{\theta}$ and $[110]_{\text{fcc Cu}}//[010]_{\theta}$, $(1\bar{1}1)_{\text{fcc Cu}}//(103)_{\theta}$.

Meanwhile, when the 1.5 Cu steel was heated to 700 °C at the rapid heating rate of 50 °C/s and gas-quenched, small Cu particles formed near cementite particles (Fig. 8c). The particles were identified as bcc Cu precipitates from the analysis of the fast Fourier transform (FFT), as shown in Fig. 8d. The bcc Cu particles are considered to be coherently precipitated in the tempered martensite matrix, and they will transform to 9R, 3R, and fcc Cu with further tempering to minimize the interfacial strain energy between the particle and the matrix [38].

Conclusions

(1) The addition of 1.5 wt% Cu to a medium C steel suppressed carbide precipitation during quenching from 900 °C, i.e., the auto-tempering effect, resulting in the large amount of solute C atoms in virgin martensite.

(2) Whereas the addition of Cu did not influence the start temperature of ε-carbide precipitation during continuous heating, it slightly delayed the finish temperature of ε-carbide precipitation and increased the amount of ε-carbide precipitates due to the suppressed auto-tempering.

(3) The addition of 1.5 wt% Cu delayed cementite precipitation during continuous heating, resulting in relatively fine cementite particles. The slow growth of

cementite particles in the 1.5 Cu steel was due to the following reasons: the partitioning of Cu atoms from cementite particles to the martensite matrix, the hindrance to the migration of cementite interfaces by Cu particles formed near cementite particles, and the slowed diffusions of C and Fe atoms.

(4) Cu precipitation in the medium C steel was accelerated by cementite precipitation because both cementite interfaces and the high Cu concentration near cementite particles provided preferential nucleation sites for Cu precipitation. The hardness of the tempered Cu-bearing medium C steel was higher than that of the tempered Cu-free steel at the tempering temperatures of over 300 °C due to both the precipitation hardening of Cu and retarded cementite precipitation.

Acknowledgements The authors gratefully acknowledge POSCO's support for materials, Pohang, Korea.

References

1. Grange RA, Lambert VE, Harrington JJ (1957) Effects of copper on the heat treating characteristics of medium-carbon steel. Trans ASM 51:377–393
2. Ikeda S, Sakai T, Fine ME (1977) Fatigue behaviour of precipitation-hardening medium C steels containing Cu. J Mater Sci 12:675–683. doi:10.1007/BF00548157
3. Bała P, Oacyna J, Krawczyk J (2007) The kinetics of phase transformation during tempering of Cr–Mo–V medium carbon steel. J Achiev Mater Manuf Eng 20:79–82
4. Olson GB, Cohen M (1983) Early stages of aging and tempering of ferrous martensites. Metall Trans A 14A:1057–1065
5. Sherman AM, Eldis GT, Cohen M (1983) The aging and tempering of iron–nickel–carbon martensites. Metall Trans A 14A:995–1005
6. Jung M, Lee SJ, Lee YK (2009) Microstructural and dilatational changes during tempering and tempering kinetics in martensitic medium-carbon steel. Metall Mater Trans A 40A:551–559
7. Caballero FG, García-Mateo C, García de Andrés C (2005) Dilatometric study of reaustenitisation of high silicon bainitic steels: decomposition of retained austenite. Mater Trans 46:581–586
8. Honeycombe RWK, Bhadeshia HKDH (1995) Steels, 2nd edn. Arnold, New York
9. Michaud P, Delagnes D, Lamesle P, Mathon MH, Levaillant C (2007) The effect of the addition of alloying elements on carbide precipitation and mechanical properties in 5% chromium martensitic steels. Acta Mater 55:4877–4889
10. Le May I, Schetky LM (1982) Copper in iron and steel. Wiley Inc., New York
11. Zhang C, Enomoto M (2006) Study of the influence of alloying elements on Cu precipitation in steel by non-classical nucleation theory. Acta Mater 54:4183–4191
12. Yang JB, Enomoto M, Zhang C (2006) Modeling Cu precipitation intempered martensitic steels. Mater Sci Eng A 422:232–240
13. Zhang C, Enomoto M, Yamashita T, Sato N (2004) Cu precipitation in a prestrained Fe–1.5 wt pct Cu alloy during isothermal aging. Metall Mater Trans A 35A:1263–1272
14. Bhagat AN, Pabi SK, Ranganathan S, Mohanty ON (2007) Study on copper precipitation during continuous heating and cooling of HSLA steels using electrical resistivity. Mater Sci Technol 23:158–164
15. Jung JG, Jung M, Lee S, Shin E, Shin HC, Lee YK (2013) Cu precipitation kinetics during martensite tempering in a medium C steel. J Alloys Compd 553:299–307
16. Saito N, Abiko K, Kimura H (1995) Effects of small addition of titanium, vanadium and chromium on the kinetics of ε-carbide precipitation in high purity Fe–C alloys. Mater Trans JIM 36:601–609
17. Zhu C, Xiong XY, Cerezo A, Hardwicke R, Krauss G, Smith GDW (2007) Three-dimensional atom probe characterization of alloy element partitioning in cementite during tempering of alloy steel. Ultramicroscopy 107:808–812
18. Miyamoto G, Oh JC, Hono K, Furuhara T, Maki T (2007) Effect of partitioning of Mn and Si on the growth kinetics of cementite in tempered Fe–0.6 mass% C martensite. Acta Mater 55:5027–5038
19. Chang L, Smith GDW (1984) The silicon effect in the tempering of martensite in steels. J Phys Colloques 45:C9-397–C9-401
20. Ishida K (1995) Calculation of the effect of alloying elements on the M_s temperature in steels. J Alloys Compd 220:126–131
21. Cheng L, Brakman CM, Korevarr BM, Mittemeijer EJ (1988) The tempering of iron–carbon martensites: dilatometric and calorimetric analysis. Metall Trans A 19A:2415–2426
22. Eppstein S, Lorig CH (1935) Note on the carburizing copper steels. Met Alloys 6:91–92
23. Irmer V, Keller-Kniepmeier M (1972) On the influence of impurity atoms on self-diffusion in α-iron single crystals. Philos Mag 25:1345–1359
24. Mittemeijer EJ, Cheng L, van der Schaaf PJ, Brakman CM, Korevarr BM (1988) Analysis of nonisothermal transformation kinetics: tempering of iron–carbon and iron–nitrogen martensites. Metall Trans A 19A:925–932
25. Cohen M (1970) Self-diffusion during plastic deformation. Trans JIM 11:145–151
26. Buffington FS, Hirano K, Cohen M (1961) Self diffusion in iron. Acta Metall 9:434–439
27. Fourlaris G, Baker AJ, Papadimitriou GD (1995) Microscopic characterisation of ε-Cu interphase precipitation in hypereutectoid Fe–C–Cu alloys. Acta Metall Mater 43:2589–2604
28. Miller MK, Smith GDW (1977) Atom probe microanalysis of a pearlitic steel. Met Sci 11:249–253
29. Ande CK, Sluiter MHF (2010) First-principles prediction of partitioning of alloying elements between cementite and ferrite. Acta Mater 58:6276–6281
30. Christian JW (1975) The theory of transformations in metals and alloys. Pergamon Press, Oxford
31. Lusk M, Jou HJ (1997) On the rule of additivity in phase transformation kinetics. Metall Mater Trans A 28A:287–291
32. Porter DA, Easterling KE (1992) Phase transformations in metals and alloys, 2nd edn. Nelson Thornes Ltd, Cheltenham
33. Maruyama N, Sugiyama M, Hara T, Tamehiro H (1999) Precipitation and phase transformation of copper particles in low alloy ferritic and martensitic steels. Mater Trans JIM 40:268–277
34. Russell KC, Brown LM (1972) A dispersion strengthening model based on differing elastic moduli applied to the iron–copper system. Acta Metall 20:969–974
35. Kim S, Lee C (2012) Behavior of Cu precipitates during thermomechanical cycling in the weld CGHAZ of Cu-containing HSLA steel. Met Mater Int 18:857–862
36. Kramer JJ, Pound GM, Mehl RF (1958) The free energy of formation and the interfacial enthalpy in pearlite. Acta Metall 6:763–771
37. Wasynczuk JA, Fisher RM, Thomas G (1986) Effects of copper on proeutectoid cementite precipitation. Metall Trans A 17A:2163–2173
38. Othen PJ, Jenkins MK, Smith GDW (1994) High-resolution electron microscopy studies of the structure of Cu precipitates in α-Fe. Philos Mag A 70:1–24